

Photoemission from Clean and Cesium-Covered Nickel Surfaces

T. A. CALLCOTT* AND A. U. MAC RAE

Bell Telephone Laboratories, Murray Hill, New Jersey 07974

(Received 15 August 1968)

Photoemission energy distributions (PED) have been measured for clean and cesium-covered single-crystal Ni(111) surfaces. The surface condition was monitored during the experiments with a low-energy electron-diffraction (LEED) apparatus. Photoemission results for the clean surface are similar to those previously reported for polycrystalline material, except that minor structure resulting from direct transitions was observed, and a much higher work function of 5.42 ± 0.04 eV was obtained for the (111) surface than has been reported for polycrystalline surfaces. The relative intensity of the anomalous peak at -4.5 eV with respect to the upper edge of the PED was found to vary with surface condition. With monolayer cesium coverage, very strong peaks are observed in the PED at -4.0 and -5.4 eV. These peaks appear when cesium is applied in excess of that required to lower the work function to its minimum value. A LEED pattern indicating ordering over twice the Ni lattice spacing is correlated with the cesium-related peaks. We argue that a fixed energy-loss mechanism is operating that causes structure to be displaced in the external PED by the amount of the fixed energy loss. We present evidence that this loss does not occur during transport of a photoexcited electron across the surface region, but that it accompanies the optical absorption process. It is suggested that peaks at -4.5 eV on clean Ni and at -4.0 and -5.4 eV on cesium-covered Ni result from the simultaneous excitation of interband transitions and a surface plasmon of 4.0 – 4.5 eV. Further experiments are suggested to check this hypothesis. For cesium coverages in excess of about three monolayers, a shoulder appears in the PED at -2.8 eV that we interpret as resulting from the excitation of the bulk plasmon in cesium.

I. INTRODUCTION

MEASUREMENTS of photoemission energy distributions (PED) from nickel have been reported for evaporated polycrystalline films¹⁻⁴ and polycrystalline samples cleaned by sputtering and subsequent annealing.⁵ In this previously reported work all structure in the PED was observed to change in energy position by the amount of the change in photon energy, i.e., to obey the relation

$$\Delta E_{\text{str}} = \Delta h\nu. \quad (1)$$

Assuming negligible⁶ energy losses in the absorption, transport, and escape processes affecting photoemitted electrons, structure that obeys (1) over a large range of photon energies reflects structure in the density of filled electron states below the Fermi level.

If an electron is excited without energy loss, its final energy is given by

$$E_f = E_i + h\nu, \quad (2)$$

where E_i is the energy of the initial state of the transi-

* Present address: Physics Dept., University of Tennessee, Knoxville, Tenn.

¹ A. J. Blodgett, Jr. and W. C. Spicer, Phys. Rev. Letters **15**, 29 (1965); A. J. Blodgett, Jr. and W. E. Spicer, Phys. Rev. **146**, 390 (1966); A. Y-C Yu and W. E. Spicer, Phys. Rev. Letters **17**, 1171 (1966).

² A. J. Blodgett, Jr., Ph.D. thesis, Stanford, 1965 Technical Report No. 5205-2 (unpublished). This thesis gives PED taken on differently prepared Ni films which do not show the anomalous peak at -4.5 eV as well as PED from cesium-covered Ni that are not discussed in the publications of Ref. 1.

³ R. C. Vehse and E. T. Arakawa, Bull. Am. Phys. Soc. **13**, 59 (1968); and (unpublished).

⁴ D. E. Eastman and W. F. Krolikowski, Phys. Rev. Letters **21**, 623 (1968).

⁵ W. M. Breen and F. Wooten, Phys. Rev. **159**, 475 (1967).

⁶ The resolution of the PED's is about 0.2 eV, so that energy losses smaller than this, including specifically single-phonon losses, are negligible for this work.

tion and $h\nu$ is the photon energy. An electron is said to have undergone an energy loss during absorption if all of the exciting photon's energy does not go into such a one-electron transition. For two or multielectron excitations where the photon energy is shared arbitrarily between two or more electrons, the concept is not very useful. It is convenient, however, if a prominent absorption mechanism involves a fixed energy loss ΔE so that many electrons escape with a final energy given by

$$E_f = E_i + h\nu - \Delta E. \quad (3)$$

Then structure in the PED can appear to be displaced by ΔE below its normal energy position.

Representative results from a polycrystalline nickel surface for photon energies to 11 eV are shown in Fig. 1.

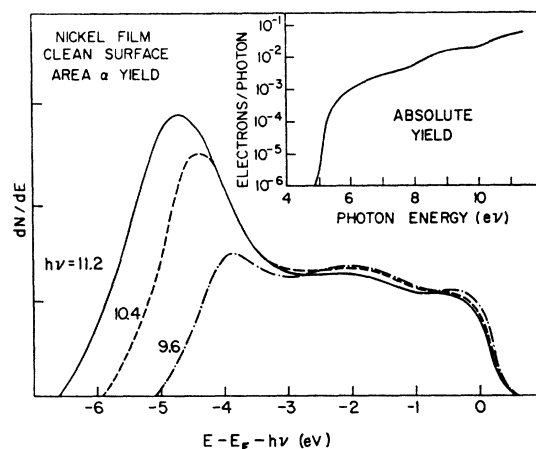


FIG. 1. Energy distributions of photoelectrons from a Ni film. Curves are labeled with incident photon energies. Data replotted from Blodgett and Spicer (Ref. 1).

Structural features are a narrow peak located at the high-energy edge of the distributions, a broad structure centered at about -2.0 eV, and a prominent peak located at -4.5 eV. In other data from evaporated films, the peak at -4.5 eV is much less prominent than that shown in Fig. 1.^{2,4} Its magnitude relative to other peaks in the energy distributions appears to depend on sample preparation and surface condition. Our results give additional support to this conclusion. Recent work on films to photon energies of 25 eV indicates that additional structural features are located at energies below -10 eV.³ We note that the energy distributions reported by Eastman and Krolikowski⁴ show sharper structure than do ours or those of other workers referred to here. It seems probable to us that this improvement in resolution results from a successful effort to improve retarding-field geometries.

The energy scale in Fig. 1 and for all subsequent PED's is $E - E_F - h\nu$, where E is the energy of the photoemitted electron, E_F is the Fermi level energy, and $h\nu$ is the photon energy. Structure obeying (1) appears stationary in energy position on this scale for all photon energies. If energy-loss processes are negligible, the energy scale gives directly the location of the initial states for the optical absorption process.

Approximately single-layer coverages of cesium on clean surfaces have been successfully used in numerous photoemission experiments to lower the work function of surfaces studied to about 1.5 eV. This allows the escape of electrons with final energies between this value and typical clean surface work functions of 4–6 eV. In most materials, structure in the PED at energies greater than about 6 eV above the Fermi level are substantially unchanged by the addition of the cesium layer; effects observed can be attributed to nearly elastic scattering of the escaping electrons from the deposited cesium. PED reported by Blodgett and Spicer for cesiated Ni films show structure similar to that from a clean surface, but the -2.0 - and -4.5 -eV peaks are shifted somewhat in energy position.² In this paper we report the effects of cesium on PED from single-crystal Ni. Strong structural features due to the cesium coverage are observed that cannot be explained by straightforward scattering mechanisms.

From their data on clean surfaces, Blodgett and Spicer derived the "optical" density of initial states of the transitions producing photoemitted electrons.^{1,7} In the absence of large energy-loss processes, this density of states should approximate the true one-electron density of states. Soft x-ray and ion-neutralization spectroscopy experiments provide independent means of estimating the state density. They show a high density of states extending to about 3 eV below the Fermi level, but no prominent structure corresponding

⁷ W. E. Spicer, Phys. Rev. **154**, 385 (1967); Dr. Spicer discusses the differences between optical and true densities of states at length in this article.

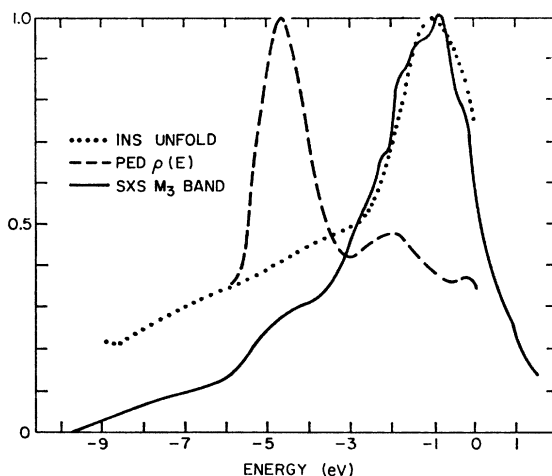


FIG. 2. Experimental curves interpreted as representing the density of filled states in Ni. The zero of the energy scale is at the Fermi level. The curves represent the ion neutralization spectroscopy unfold function (Ref. 9), the M_3 emission band in soft x-ray spectroscopy (Ref. 8), and the "optical" density of states derived from photoemission energy distributions (Ref. 1). The curves are normalized at their maxima. This drawing is reproduced from Ref. 8.

to the photoemission peak at -4.5 eV.^{8,9} Densities of states calculated from theoretical band structures show a similar structure with a high density of d electrons extending to about 4 eV below the Fermi level and a much smaller density of electrons extending to lower energies.¹⁰ Various experimental results that are interpreted as showing the density of filled states in Ni are exhibited in Fig. 2. Very recent photoemission results⁴ give a PED derived density of states in which the low-energy peak is much less pronounced than in Fig. 2. It appears as a low-energy shoulder of smaller magnitude than the peaks at 0 and -2 eV. It seems clear from these results that some effect related to the surface condition is responsible for the -4.5 -eV peak and that it does not reflect simply a maximum in the one-electron density of states.

Several attempts have been made to explain the -4.5 -eV peak on some basis other than a one-electron density-of-states effect.^{11–13} The suggestion of Nesbet and Grant¹³ is particularly relevant to our interpretation of the Ni data. They suggest that excited electrons undergo a fixed energy loss of $\Delta E \approx 4.5$ eV during the

⁸ J. R. Cuthill, A. J. McAlister, M. L. Williams, and R. E. Watson, Phys. Rev. **164**, 1006 (1967).

⁹ H. D. Hagstrum and G. E. Becker, Phys. Rev. **159**, 572 (1967); H. D. Hagstrum and G. E. Becker, Phys. Rev. Letters **16**, 230 (1966).

¹⁰ J. W. D. Connolly, Phys. Rev. **159**, 415 (1967); L. Hodges, H. Ehrenreich, and N. D. Lany, *ibid.* **152**, 505 (1966); many additional references are given in these papers.

¹¹ J. C. Phillips, Phys. Rev. **140**, A1254 (1965).

¹² N. F. Mott, in *Proceedings of the Symposium on Optical Properties and Electronic Structure of Metals and Alloys*, edited by F. Abeles (North-Holland Publishing Company, Amsterdam, 1966), p. 314.

¹³ R. K. Nesbet and P. M. Grant, Phys. Rev. Letters **19**, 222 (1967).

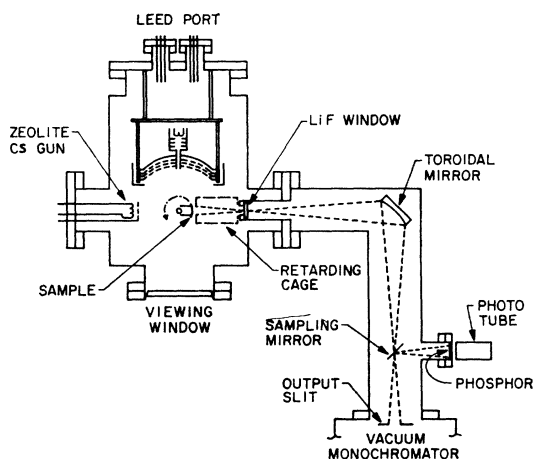


FIG. 3. Schematic diagram of experimental apparatus. The sample may be rotated to face all ports.

absorption process. This loss is identified with the loss of about 4.5 eV that monoenergetic electrons suffer in traversing a thin Ni film. The loss produces a shoulder in energy-distribution curves taken after the electrons have traversed a Ni film.¹⁴ A stronger peak in the characteristic energy-loss data indicates a loss of 10 eV. Vehse and Arakawa³ identify this loss as the volume plasma excitation and invoke this loss mechanism to explain structure that they observe below -10 eV in PED's taken at photon energies as high as 25 eV. In their explanation, structure produced in the optical excitation process appears in the external distributions displaced in energy by the amount of the fixed energy loss. Losses occurring during absorption and during transport cannot, of course, be rigorously separated. The concept is useful, however.

A fixed energy loss can occur during the optical excitation process when the photon produces a single-electron transition and a plasma excitation. Several theorists have estimated that the strength of plasma excitation processes are small in comparison to other absorption mechanisms,¹⁵⁻¹⁷ except possibly in the case of the alkali metals.¹⁷ It seems likely, however, that processes involving the excitation of a surface plasmon, while making a small contribution to the total absorption, can contribute significantly to excitations occurring near the surface. When the escape depth of excited electrons is small in comparison to the absorption depth of incident light, such surface-related processes can be far more important in photoemission than in experiments that monitor the total absorption. Eastman and Krolikowski⁴ have estimated, on the basis of an analysis of photoemission results as a function of Ni

film thickness, that the scattering length for large energy loss processes in Ni is very short (5–15 Å) and that few photoexcited electrons escape from depths greater than about 30 Å.

Our experiments incorporated three improvements over previously reported experimental studies. The experiments were performed on a single-crystal Ni surface; low-energy electron-diffraction (LEED) equipment was used to monitor the surface conditions, and a cesium source capable of depositing controlled and measurable small cesium coverage was used. These factors allowed us to monitor surface conditions more closely than in previous experiments. This does not imply that our photoemission results are necessarily better than those of other workers, but only that they are taken on more accurately defined surfaces. We have previously noted that the resolution of PED taken by Eastman are superior to ours, probably as a result of better retarding field geometries.

We believe that the results presented here shed light on many of the problems encountered in attempting to explain the photoemission results from clean and cesium-covered Ni. We conclude from our data that (a) PED from single-crystal and polycrystalline Ni samples are very similar, (b) the two high-energy peaks in the PED are produced by one-electron transitions without large energy loss and that at least a small, but measurable fraction of these are direct transitions, (c) that the photoemission peak at about -4.5 eV is associated with a fixed energy-loss process occurring near the surface, (d) that this energy loss accompanies optical absorption in the surface region and does not occur when electrons excited deep in the sample pass through the surface region, (e) that surface contaminants and in particular small cesium coverages (≤ 1 atomic layer) strongly modify the loss process occurring near the surface in Ni, and (f) that for large cesium coverages (\geq three layers), an absorption process involving a fixed energy loss of -2.8 eV occurs in the cesium layer. Arguments are presented that the fixed energy losses result from plasma excitation processes.

II. EXPERIMENTAL PROCEDURES

Data reported here were taken on the (111) surface of a single-crystal Ni sample. The sample was electropolished to a mirror finish and electroetched outside the vacuum using techniques detailed elsewhere.¹⁸ It was then sputter cleaned with argon and heated in vacuum to obtain a sharp LEED pattern reflecting the symmetry and lattice spacing of bulk Ni. Subsequent recleaning of the surface could usually be accomplished by heating alone.

The experiments were performed in a LEED system which was modified by installing a LiF window to admit uv light and a retractable cylindrical retarding poten-

¹⁴ J. L. Robins and J. B. Swan, Proc. Phys. Soc. (London) **76**, 857 (1960).

¹⁵ R. H. Ritchie, Surface Sci. **3**, 497 (1965).

¹⁶ Peter A. Fedders, Phys. Rev. **165**, 580 (1968).

¹⁷ R. J. Esposito, L. Muldrew, and P. E. Bloomfield, Phys. Rev. **168**, 744 (1968).

¹⁸ A. U. Mac Rae, Surface Sci. **1**, 319 (1964).

tial cage used for the photoemission measurements. A schematic of the experimental layout is shown in Fig. 3.

Light for our photoemission measurements is produced by a Jarrell-Ash 0.5 m Ebert vacuum monochromator equipped with MgF-coated optics and a windowless Hinteregger-type hydrogen source. The exit slit is refocused on the sample by a MgF-coated toroidal mirror. Light intensity is monitored by deflecting a small portion of the exit beam to a sodium salicylate phosphor monitored by a phototube. The system is not adequately calibrated to give reliable comparisons of photon fluxes at widely separated wavelengths. At a fixed wavelength, the sensitivity of the light-monitoring system remains constant within a few percent during the one-day running periods normally required to complete a given experiment.

Photoemission current to the sample is measured with a Cary 31 electrometer. PED's are measured using a retarding potential method; as a ramp voltage is applied between the sample and the retarding potential cage, the output of the electrometer is electronically differentiated and plotted against the ramp voltage on an X - Y recorder. This gives directly the relative numbers of electrons as a function of energy in eV. The energy resolution of the measurements are estimated to be about 0.2 eV at photon energies of 10 eV and somewhat better at lower photon energies. Further details of the measurement technique and the resolution obtainable have been given elsewhere.¹⁹

The energy scale of the external electrons is set with respect to the solid's energy-band parameters by assigning the upper edge of the PED an energy of $E_F + h\nu$. The assignment is considered to be accurate to 0.1 eV.

Cesium was applied to the sample surface with an atomic beam gun for heavy coverages and with a zeolite-type cesium ion gun for light coverages.²⁰ For the latter, coverage was determined by measuring the ion current reaching the sample. The coverage obtained in this way assumes a sticking coefficient of 1, no deposition of neutral cesium onto the sample, and no re-evolution of neutral cesium into the vacuum. The assumptions are approximately valid for the first atomic layer of cesium. With heavy coverages, cesium readily evaporates into the vacuum. Uncertainties due to the collection of cesium on the heavy supporting leads necessary for heating were minimized by shielding and a calibration experiment using a dummy sample that allowed current to the face of the sample and to other surfaces to be measured separately.

Absolute work-function measurements were made by extrapolating the square root of the yield to zero,²¹ as illustrated in Fig. 4. Work functions obtained in this way are given to three significant figures in this paper.

¹⁹ T. A. Callcott, Phys. Rev. **161**, 746 (1967).

²⁰ R. E. Weber and L. F. Cordes, Rev. Sci. Instr. **37**, 112 (1966).

²¹ R. H. Fowler, Phys. Rev. **38**, 45 (1951).

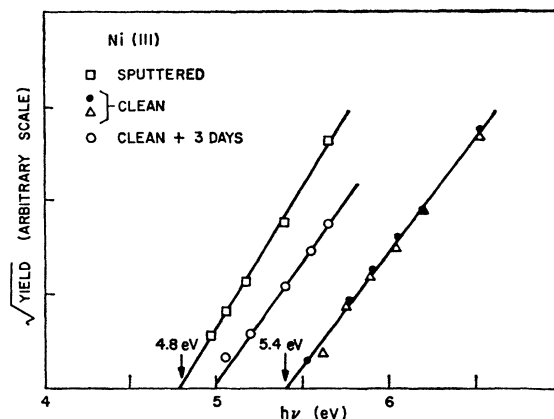


FIG. 4. $(\text{Yield})^{1/2}$ extrapolated to zero to obtain work function of Ni surfaces after various surface treatments.

The accuracy of the work function determined in this way depends directly on the resolution of the monochromator used as a light source, and on the assumption that the response of the uv detector is nearly flat within a range of about 1 eV above the photoemission threshold. Most measurements were taken with slit openings of 1 mm, which gives a linear dispersion of 15 Å and a resolution at 0.03–0.05 eV in the photon energy range 5–6.5 eV. One measurement of spectral yield was taken with 0.4-mm slit openings to improve this resolution to $\leq .02$ eV. Sharp variations in detector response with time or photon energy would have been immediately detected since the hydrogen arc lamp used as a light source produces a well-behaved continuum in this spectral region. Changes in work function during cesium deposition and heating were usually monitored by measuring the energy shift of the low-energy edge of the PED's taken at a fixed photon energy.¹⁹ Values of the work function obtained in this way are given to 0.1 eV in this paper. The shifts were taken with respect to a PED measured on a surface for which a work function obtained from the extrapolated yield was available.

Some of these experiments were performed under relatively poor vacuum conditions at pressures of 1 to 3×10^{-9} Torr, others at a pressure of about 2×10^{-10} Torr. An attempt was made to make measurements as rapidly as possible after flashing the crystal to minimize the effects of contamination. Nevertheless, as the discussion below makes clear, some contamination of the surfaces occurred in the poorer vacuum. We do not believe that these contamination problems affect the qualitative features of the photoemission data or the conclusions drawn from the data.

III. EXPERIMENTAL RESULTS

A. LEED and Work-Function Results on "Clean" Surface

Figure 4 shows extrapolated yield plots of data taken on several sample surfaces. The clean-surface plots are

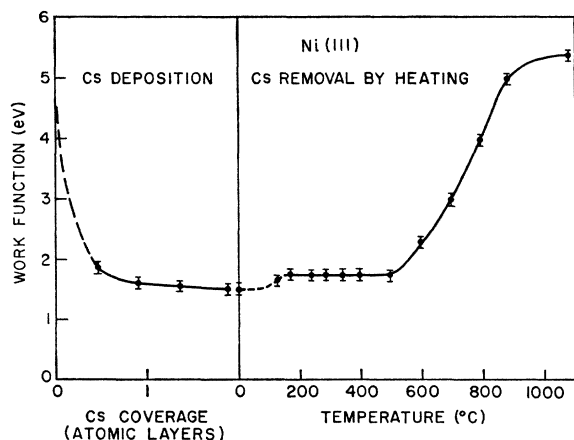


FIG. 5. Work-function changes observed during deposition of cesium and after heating the sample momentarily to the temperatures indicated.

typical of those obtained when yield plots are made within a few minutes after annealing a sputtered surface to 880°C and obtaining a clean LEED pattern. The other plots were taken after sputtering but before annealing, and after the annealed surface had remained undisturbed in a 10^{-9} Torr vacuum for three days. A work function value of 5.42 ± 0.04 eV was found in this and other similar measurements to be characteristic of the atomically clean Ni(111) surface. All surfaces prepared in the above fashion showed work-function values falling within this range. Values of 4.5–5.0 eV have been reported for polycrystalline surfaces.¹⁻⁵ Such differences are to be expected between values obtained from individual low-index faces of single-crystal metals and from films, where surfaces represent some average over various crystal faces. We know of no other experimental values of the work function for a (111) face of Ni. Our results may be compared with the theoretical predictions of Steiner and Gyftopoulos,²² who calculate a value of 5.56 eV for this face.

In another experiment, in a system vacuum of 5×10^{-9} Torr, the work function increased with time to a value of about 5.55 eV after 10 min and then decreased slowly to a stable value of 5.0 eV after 24 h. No detectable change in the LEED pattern was observed during the initial increase in the work function. The stable value of 5.0 eV was associated with a diffuse background added to the characteristic Ni pattern. Heating the sample to 880°C restored both the original work function and the LEED pattern.

Designation of a surface as atomically clean is ambiguous at best. Here we mean a surface with a sharp LEED pattern characteristic of the Ni(111) surface and a work function of 5.42 eV. These are the conditions obtained by electroetching in air, sputtering

in a 10^{-4} Torr argon atmosphere, and annealing the sputtered surface to 880°C in ultrahigh vacuum. After contamination with system gases (probably mostly CO) changes the work function and fuzzes the LEED pattern, the clean condition can be restored by heating the sample to 880°C.

B. LEED and Work-Function Results on Cs-Covered Surfaces

Detailed LEED results on the cesium-covered Ni surface will be reported elsewhere.²³ Briefly, they are that the first cesium layer goes down with ordering over twice the lattice spacing of the Ni substrate (a 2×2 structure). Thus a layer of cesium requires $\frac{1}{4}$ the number of atoms in a layer of the Ni substrate. In experiments performed in the 10^{-9} Torr vacuum, spots appeared in the LEED pattern after the deposition of additional cesium, indicating ordering over four lattice spacings. In the 10^{-10} Torr vacuum, the 2×2 structure was the only LEED pattern obtained. Both LEED structures appeared after deposition to be accompanied by a diffuse background, but were rendered sharp by momentary heating to about 300°C.

The behavior of the work function during cesium deposition in a vacuum of 2×10^{-10} Torr and subsequent heating is shown in Fig. 5. Here one atomic layer of cesium is taken equal to 4.65×10^{14} atoms/cm², which is $\frac{1}{4}$ the number of surface atoms on the (111) face of Ni. The calculated coverage is estimated to be accurate to $\pm 20\%$. A minimum value of 1.5 eV was obtained after deposition. A slightly higher value of 1.7 eV was associated with the sharp 2×2 LEED pattern obtained with minor heating. Very similar results were obtained for the 4×4 structure produced in poorer vacuum except that the work function associated with this structure was 1.8 eV. After heating to 600°C the work function begins to rise but only reaches its clean-surface value after heating to 1000°C. After the 600°C heating, however, the LEED pattern is a sharp 1×1 structure indistinguishable from that obtained from the clean Ni surface. From the disparity in the heat treatment necessary to produce a clean-surface LEED pattern and a clean-surface work function, it is obvious that LEED patterns are not sensitive to small densities of cesium surface atoms.

The possible significance of much of this is discussed elsewhere.²³ For our present purposes, we note the striking correlation between the work function value of 1.7 eV and the 2×2 cesium superstructure. This correlation extends still further to structure in the PED (peaks 4 and 6) which will be discussed in Sec. III D. We find that the LEED structure and the structure in the PED appear faintly at a coverage of about $\frac{3}{4}$ layer as the work function approaches its minimum value during cesium deposition. The LEED pattern is weak

²² D. Steiner and E. P. Gyftopoulos, in Proceedings of the Twenty-Seventh Conference on Physical Electronics, Boston, 1967, p. 160 (unpublished).

²³ A. U. Mac Rae and T. A. Callcott (unpublished).

and the cesium-related peak 6 is depressed after momentary heating to 500°C. Both disappear after heating the sample to 600°C.

In a general way, it was observed that whenever LEED spots were diffuse or a strong background accompanied the LEED pattern, the photoemission yields were lower and the structure was somewhat washed out. These effects result from elastic scattering of electrons from disordered atoms on the sample surface.

Multilayer coverages of cesium deposited in 10^{-10} Torr vacuum had a work function of 1.5 eV. Other workers have found that when cesium is deposited on many metals, the work function goes through a minimum of 1.5 eV at monolayer coverage or less and then rises to a final value of 1.8 eV, believed to be characteristic of bulk cesium.²⁴ We observed no such rise in work function at higher coverages. In a 10^{-9} -Torr vacuum, a higher work function of about 1.8 eV was observed after cesium deposition. LEED pattern showing ordering over four lattice spacings (the 4×4 structure) accompanied the higher work function values.

Assuming that the 1.8-eV value for the work function of bulk cesium is correct, the lower value that we obtain for multilayer coverage may be significant. The method of monitoring the work function by measuring energy shifts of the lower edges of the PED is not highly precise for several reasons, but, if care is taken to avoid variation of the collector work function, it should not produce errors as large as 0.3 eV. Photoemission measurements give the lowest surface work function rather than the average work function given by contact potential measurements. Consequently, uneven or

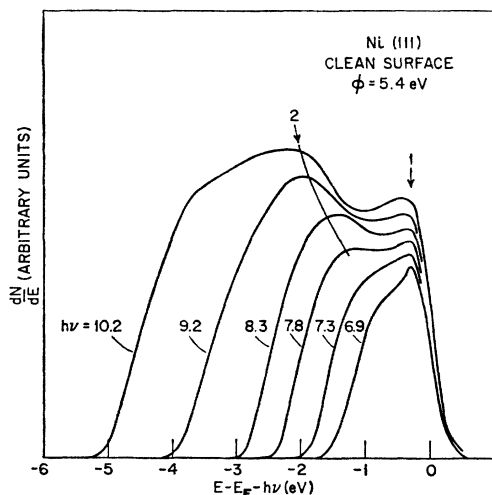


FIG. 6. Energy distributions from a clean (111) face of Ni. Curves are labeled with incident photon energies. Numbered arrows indicate structure discussed in text.

²⁴ H. Mayer and B. Hietel, in *Proceedings of the Symposium on Optical Properties and Electronic Structure of Metals and Alloys*, edited by F. Abeles (North-Holland Publishing Co., Amsterdam, 1966), pp. 47-59.

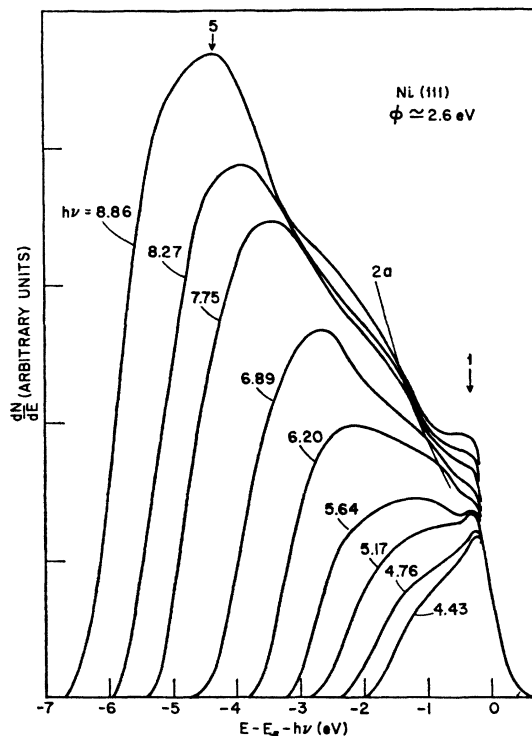


FIG. 7. Energy distribution from a Ni surface with fractional monolayer coverage of cesium. Curves are labeled with photon energies. Numbered arrows indicate structure discussed in text.

patchy cesium coverage could account for the discrepancy. If further studies show that the discrepancy is real, then it is important because it suggests that a mixing of cesium and Ni occurs at the surface that prevents the buildup of cesium on the surface. Possible consequences of such mixing will be mentioned briefly in succeeding sections of this paper. The first such possible consequence is that the ordered cesium layer is made up of alternately placed cesium and Ni atoms. Assuming interatomic distances the same as those of the Ni substrate, such an arrangement requires twice as much cesium per layer as we have used in calculations of the number of monolayers.

C. Structure in PED Characteristic of "Clean" Nickel

PED taken on a clean surface at photon energies from 6 to 10 eV are shown in Fig. 6. Curves in this figure, and in Figs. 7 and 8, are not normalized to yield. Since we do not have accurate yield values in the photon energy range 6-10 eV, we have plotted the PED so that they do not overlap. Assuming that the response of the uv detector is flat, this procedure causes a small increase in the size of the PED with increasing photon energy. Assuming a flat response, we observe that the number of electrons escaping at the high-energy edge of the PED is approximately constant for photon energies above 6 eV. Two structural features may be noted in Fig. 6, a narrow peak at the upper edge of the

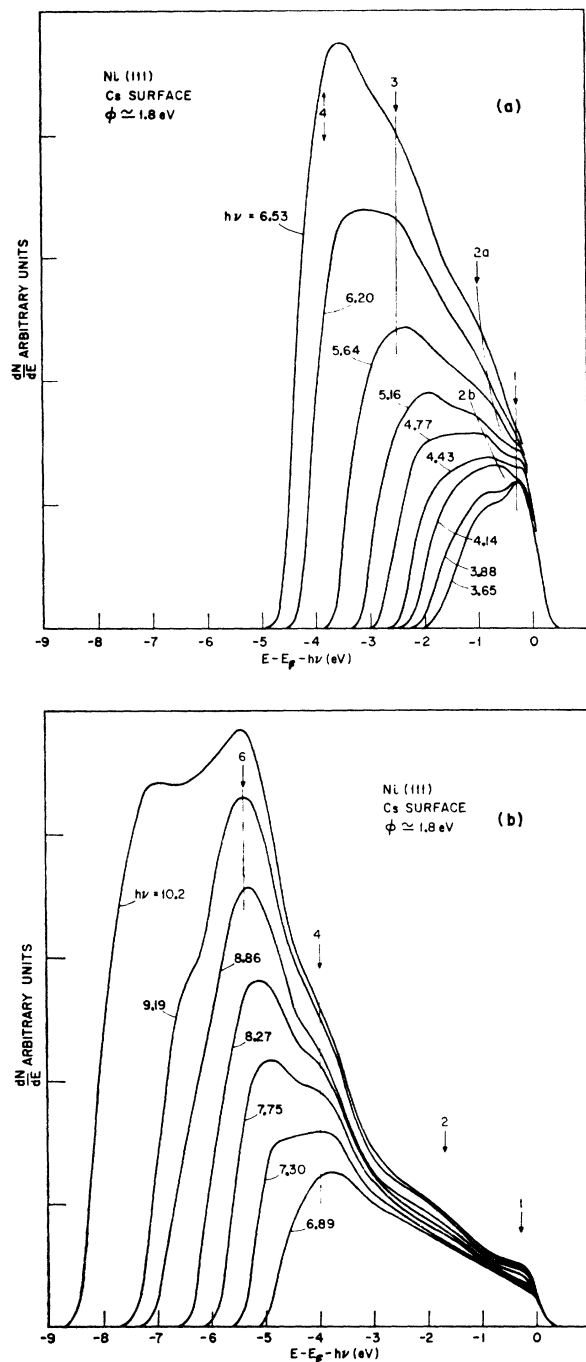


FIG. 8. Energy distributions from a Ni surface after deposition of approximately two monolayers of cesium. Curves are labeled with photon energies. Numbered arrows indicate structure discussed in text.

distribution and a broad central maximum which is uncovered as the photon energy increases from 7 to 10 eV. Sufficient photon energy is not available to allow electrons in a peak at -4.5 eV to surmount the surface barrier.

PED from a lightly cesiated sample are shown in Fig. 7 for photon energies of 4.4–8.9 eV. These data were taken after a cesiated surface was heated to 700°C . Similar data have been obtained after light cesiation (~ 0.3 monolayers) without heating. The peak at the high-energy edge of the distributions is present at all photon energies. The broad central structure shows a structural feature that is not stationary on this plot and so does not obey relation (1). A shoulder appears at the upper edge of the structure for photon energies between 5 and 6 eV and moves away from the edge with increasing photon energy. Electrons in this shoulder are lost under a broad stationary structure centered at -2.5 eV and form a smooth central peak at photon energies $\gtrsim 8$ eV. Peak 5 at -4.5 eV is identified with the anomalous, low-energy peak discussed in the Introduction.

Figures 8(a) and 8(b) show PED from a fully cesiated surface prepared by deposition of several layers of cesium, for photon energies of 3.6–10.2 eV. These measurements were made in a 10^{-9} Torr vacuum and LEED showed the 4×4 superstructure described above. Very similar curves have been obtained with surfaces showing the 2×2 LEED pattern except that lower work functions were obtained. The shoulder mentioned in the preceding paragraph is visible here between photon energies of 5.5 and 8.0 eV and is labeled 2a. A second weak shoulder appearing at lower photon energies is labeled 2b. The broad peak labeled 3 is stationary in energy position. At photon energies above 8 eV, the several minor structural features can no longer be resolved and appear as the single broad maximum labeled 2 in Fig. 8(b). Peak 3 is thought to be a weak indication of a strong shoulder associated with heavy cesium coverage that is discussed further below.

We believe that structural features 1 and 2 are produced by transitions from electronic states lying in a group of closely spaced bands extending to 3 or 4 eV below the Fermi level. The presence of some minor structure in peak 2 that moves with photon energy but does not obey (1) indicates that direct transitions make a contribution to the electrons appearing in these peaks.¹⁸ The multiplicity of closely spaced bands and the limited resolution of the PED's makes it unlikely that the contributions of direct and nondirect transitions in this energy region can be separated.

D. Structure in PED Associated with Cs-Covered Ni

Structures 4 and 6 located at -4.0 and -5.4 eV in Fig. 8(b) are associated with cesium coverage. They are larger in magnitude and straddle the energy position of the -4.5 -eV peak observed at smaller cesium coverages. At photon energies where peak position is unaffected by the probability of the escape function, both peaks are stationary in energy position and so obey relation (1).

Figure 9 shows the effect of the deposition of cesium on the PED at a fixed photon energy of 9.2 eV. The curves are labeled with cesium coverages in monolayers. The absolute values given are of doubtful accuracy since a calibration run using a dummy sample was not made for this experiment. The coverage scale was adjusted by a constant multiplying factor to bring it into reasonable agreement with the coverage-versus-work-function behavior observed in well-calibrated experiments. At coverages less than one layer, the work function is progressively decreased to a value of about 1.8 eV. Peaks 1, 2, and 5 previously described are uncovered. With additional cesium coverage a strong peak (No. 6) grows at -5.4 eV. The weaker structure at -4.0 eV visible in Fig. 8(b) is poorly resolved until the sample is heated slightly. Its position is indicated by the number 4. Finally, with multilayer cesium coverage, a shoulder labeled 3 appears at -2.8 eV. Data to be presented later indicate that this results from optical excitation in the cesium layer itself.

We draw the reader's attention to several features of Fig. 9. They are, first, that structure 6 and its poorly resolved companion 4 appear only after the work function has been reduced to near its minimum value. Thus their strength appears to be proportional to the amount of cesium in excess of that required to produce the surface dipole layer. This may mean that the strength of these peaks increases with the density of electrons in the cesium layer, since this density builds up to normal cesium metal density only after the surface dipole is established. Second, we note that these curves are plotted with area proportional to yield. It is clear that the growth of peaks 4 and 6 is not accompanied by a corresponding decrease in the number of electrons escaping at a higher energy. This effectively eliminates the possibility that electrons appearing in peaks 4 and 6 are excited to higher energy in the Ni and suffer a fixed energy loss in escaping through the surface layer. Such a mechanism would require that electrons contributing to these peaks would previously have been escaping at higher energies. Finally, we recall that the LEED structure associated with monolayer cesium coverage and peaks 4 and 6 in the PED both appear under the same conditions of cesium deposition and heat treatment. This point was discussed in Sec. II B.

Figure 10 shows peaks 4 and 6 after cesium deposition and subsequent heating to about 250°C to sharpen the structure, and after heating to about 550°C to remove the cesium-related peaks. Note that the work function is still near its minimum value after raising the sample to the higher temperature. With further heating the work function begins to rise, but no further changes of the magnitude of peaks 1, 2, and 5 are observed. The dashed curve is obtained by subtracting the two curves and clearly reveals the presence of two structural features separated by about 1.4 eV. This may not be a valid means of analyzing the data since we have not

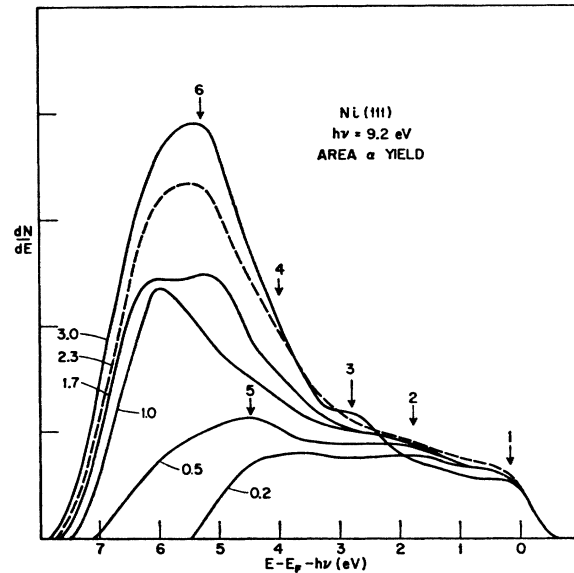


FIG. 9. Energy distributions taken at $h\nu=9.2$ eV for various cesium coverages. Area under curves plotted proportional to yield. Curves are labeled with the cesium coverage in monolayers. Cesium coverages indicated are approximate. Numbered arrows identify structure discussed in text.

determined if peak 5 is independent of peaks 4 and 6. Again we note that as peaks 4 and 6 disappear, there is no significant increase in the number of electrons escaping at higher energy.

Figure 10 shows results obtained on a sample in a 10^{-9} -Torr vacuum. Figure 11 shows the results of a similar experiment performed in a 10^{-10} -Torr vacuum.

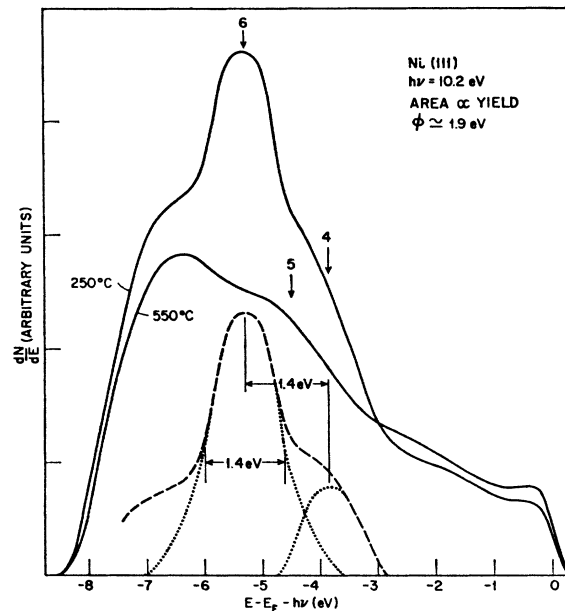


FIG. 10. Energy distributions at $h\nu=10.2$ eV after heating cesiated Ni surface to temperatures shown. Numbered arrows indicate structure discussed in text.

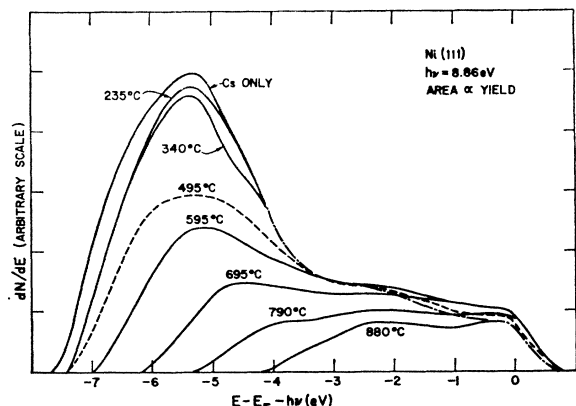


FIG. 11. Energy distributions at $h\nu = 8.9$ eV after deposition of two monolayers of cesium and after momentary heating to the temperatures indicated.

Curves at successive heating stages are shown and illustrate that the cesium-related peaks are very similar despite the differences in LEED pattern associated with the two surfaces. The double-peak structure is fully resolved only after heating to about 300°C . We believe that the resolution of structure in these curves was impaired by the slight cesium contamination of the retarding potential cage. The low-energy shoulder in Fig. 10 is not visible because the curves were taken at a lower photon energy of 8.9 eV.

The data on cesium coverage together with the LEED results strongly indicate that the 2×2 surface superstructure is associated with a single layer of cesium. The structure appears at coverages of less than one monolayer and reaches full intensity at coverages between one and two monolayers. Heating sharpens the structure, presumably by assisting in the ordering of the cesium and by driving off cesium in excess of one monolayer. Some reduction in the number of electrons

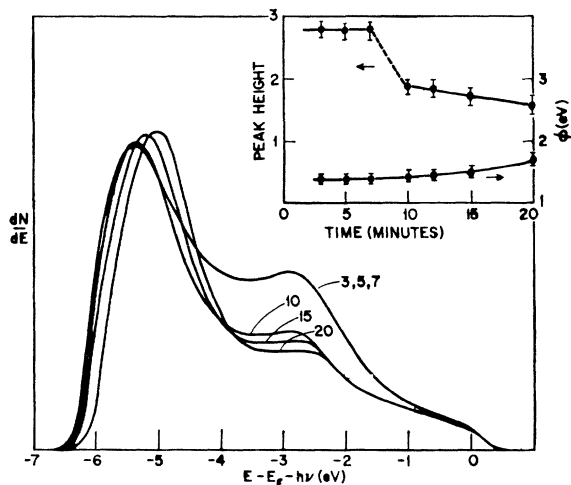


FIG. 12. Energy distributions at $h\nu = 8.9$ eV from Ni surface with multilayer cesium coverage. Numbers on curves refer to elapsed time after deposition in minutes.

in peaks 4 and 6 is observed after heating to 300°C to produce maximum sharpness in the LEED pattern, but the major effect is to more clearly resolve the two cesium-related peaks. The LEED results indicate that increased resolution results from a reduction in scattering due to surface disorder.

Blodgett and Spicer suggested that the effects they observed in cesiated Ni films resulted from alloying of the cesium and Ni over sufficient depths to produce photoemission characteristic of the alloy rather than of Ni.² Our measurements of cesium coverage, together with the LEED results, indicate that if alloying occurs, it occurs in a 1-to-1 ratio and extends to no more than one or two atomic layers.

Figure 12 gives further information about shoulder 3 at -2.8 eV associated with heavier cesium coverage and previously identified in Fig. 9. These data were taken at 7.76 eV after the deposition of many layers of cesium with the atomic beam gun. LEED patterns showed no structure. The PED was repeatedly traced as a function of time following the deposition. No change was observed for 7 min; but in the trace taken at 10 min there was a sharp decrease in the number of electrons under the shoulder followed by a slower decrease with additional time. The vapor pressure of cesium is greater than the 10^{-9} -Torr vacuum of the experiment, so that cesium is continuously evaporated from the deposited layer. In view of this, we interpret the results as indicating that below a critical film thickness the shoulder rapidly decreases in strength. After 10 min, further decreases occur more slowly and there is a slight shift in the upper edge of the shoulder from -2.8 to -2.5 eV. All curves remain within the envelope of the original trace, however. There is a shift in the work function of about 0.3 eV between the curves taken at 10 and 20 min. The origin of this shift is not certain. It may result from a concentration of nonvolatile impurities in the remaining cesium as cesium evaporates into the vacuum. In other experiments, the shoulder was reduced within about 5 min to a faint bulge like that designated 3 in Fig. 8(a). From Fig. 9 we see that the shoulder appears strongly after deposition of about three atomic layers. The electrons under the shoulder do not appear at higher energies as this shoulder weakens. Finally, though the point is not illustrated here, we note that the shoulder obeys relation (1) and moves in energy position by the amount of the change in the photon energy.

E. Summary of Experimental Results

We summarize here the conclusions drawn rather directly from the experiments about structural features 3-6. These conclusions will be discussed in the following section.

Surfaces with cesium coverages of less than one atomic layer and having work functions above 2.0 eV yield PED's having the same qualitative features as those

obtained from clean surfaces except that the work function is lowered. We find, in agreement with previous workers, the peak designated number 5. This peak:

- (1) has its maximum at -4.5 eV,
- (2) obeys the relation $\Delta E_{str} = \Delta h\nu$,
- (3) has a strength which depends on surface condition, and
- (4) LEED patterns for surfaces showing this peak can be identical to those obtained from clean (111) surfaces of Ni.

For light cesium coverages \gtrsim one atomic layer of cesium, we find two peaks (Nos. 4 and 6) with the following properties:

- (5) They have maxima at -4.0 eV (No. 4) and -5.4 eV (No. 6).
- (6) They are much stronger than peak 5 of the "clean" surface and they straddle the clean-surface peak in energy position.
- (7) They obey the relation $\Delta E_{str} = \Delta h\nu$.
- (8) Their strength relative to other structure is proportional to the amount of cesium deposited in excess of that necessary to establish the surface dipole and reduce the work function to its minimum value.
- (9) Electrons appearing in these peaks do not appear at higher energies when the peaks are suppressed by removing cesium.
- (10) There is a correlation between an ordered LEED pattern characteristic of cesium on Ni and these peaks, in that both appear at the same coverage during deposition and disappear at the same annealing temperature when cesium is driven off by heating.

For cesium coverage of \gtrsim three atomic layers, a shoulder (No. 3) appears which has the following properties:

- (11) It is located at -2.8 eV.
- (12) It obeys the relation $\Delta E_{str} = \Delta h\nu$.
- (13) Its strength depends on a critical film thickness.
- (14) Electrons do not appear at higher energies as the intensity of this peak decreases.
- (15) The surface producing this shoulder shows no ordered LEED pattern.

IV. DISCUSSION

A. Multilayer Cs Coverage

Consider first the shoulder associated with multilayer cesium coverage. We believe that this results from photoexcitation occurring in the cesium layer itself, either accompanied by or followed by a fixed energy loss of about 2.8 eV to a plasma oscillation in the cesium. The shoulder simply represents the high-energy edge of the PED displaced to lower energy by the amount of the plasma loss.

The Clausthal group has measured photoemission yields from cesium films as a function of film thick-

ness.²⁵ At a photon energy of 3.4 eV, they find that the yield saturates at a few monolayers. They interpret this as indicating a scattering length of $\lesssim 10$ Å for the production of a plasmon by an excited electron. The plasmon scattering length remains approximately constant for energies $\gg E_F + \hbar\omega_p$, where E_F is the Fermi level and $\hbar\omega_p$ is the plasmon energy. These data strongly support our contention that photoemission from thick cesium films on Ni measures electrons generated in the cesium film itself, rather than in the Ni substrate.

Without energy losses, photoemission from cesium would produce electrons with final energies within 1.7 eV of the top of the PED since the conduction band of cesium extends only about 1.7 eV below the Fermi level.²⁶ When energetically possible, plasma excitation provides the most efficient energy-loss mechanism for excited electrons in metals. The plasma loss in bulk cesium has been measured to be 2.85 eV and the surface loss has a somewhat smaller value.²⁷ This value agrees well with the fixed energy shift observed in our data. The bulk loss is suppressed and its energy shifted as the film thickness falls below a critical thickness related to the plasma wavelength.^{28,29} Surface losses also undergo shifts in energy as the film becomes very thin. These effects probably account for the suppression of shoulder 3 and the shift of its upper edge as the cesium film evaporates. This energy-loss effect with an energy characteristic of cesium gives us some confidence that a cesium-nickel alloy is not being produced at the surface.

The fact that no electrons appear at higher energies as the shoulder is suppressed suggests that it may be incorrect to view the plasma excitation as a transport loss that effects electrons equally irrespective of whether they are produced in the film or the Ni substrate. When a transport-loss mechanism is suppressed, electrons previously effected by the loss should appear at higher energies. Our evidence suggests then that an absorption mechanism producing a one-electron transition plus a plasma excitation is suppressed as the film thins. Calculations by Esposito *et al.*¹⁷ for the alkali metals indicate that plasmon-assisted intraband transitions are an important absorption mechanism in alkali metals. It may be that plasmon-assisted inter-

²⁵ H. Mayer, in Proceedings of the Symposium on Electrical and Magnetic Properties of Thin Metallic Layers, Lenven, Belgium, 1961, pp. 9-29 (unpublished); S. Methfessel, Z. Physik **147**, 442 (1957).

²⁶ F. S. Ham, Phys. Rev. **128**, 82 (1962); **128**, 2524 (1962).

²⁷ H. Mayer and B. Hietel, in Proceedings of the Symposium on Optical Properties and Electronic Structure of Metals and Alloys, edited by F. Abeles (North-Holland Publishing Company, Amsterdam, 1966), pp. 47-59.

²⁸ H. Raether, in Springer Tracts in Modern Physics (Springer-Verlag, Berlin, 1965) Vol. 38, pp. 84-157. This review paper gives a summary of solid-state plasma effects, and serves as an annotated bibliography to earlier work in the field.

²⁹ D. Pines, Elementary Excitations in Solids (W. A. Benjamin, Inc., New York, 1963), Chap. 4. This contains many references to earlier work.

band transitions are also important. Such a conclusion is perhaps to be suspected from earlier results that indicated a mean free path for the generation of plasmons of the order of a lattice spacing. For such a strong interaction between final-electron states and the plasma excitation, "indirect" transitions with plasmons replacing phonons might be indicated.

The shoulder observed in PED from thick cesium films is largely unrelated to structure observed in data from Ni, since it reflects a plasma loss in the cesium layer. The data are discussed here because of their intrinsic interest and because they clearly illustrate the effect of a plasma-loss mechanism on the PED, a theme that we will meet again in the discussion of photoemission from cesium-covered Ni. The results are not analyzed in detail because the poorly controlled experiments on thick films leave many questions unanswered. They do suggest, however, that photoemission and optical-absorption studies of the alkali metals can very profitably be extended into the vacuum ultraviolet. Particularly intriguing is the possibility that plasmon-assisted optical absorption will prove an important mechanism affecting both the optical constants and photoemission.

It would be very interesting to determine if peak 6 at -5.4 eV disappears at large cesium coverages where all photoemission can be safely attributed to the cesium layer. If this peak results from excitation near the Ni surface, as we argue below, then it should disappear at large coverages. At coverages that we have attained, the peak has not been greatly suppressed. In order to examine this question more closely, it will be necessary to cool the Ni substrate so that deposited cesium will not rapidly re-evaporate.

B. Single-Layer Cs Coverage

Cesium-related peaks 4 and 6 result from the deposition of approximately one atomic layer of cesium and thus must be considered surface phenomena. The experimental results rule out several of the possible processes through which the surface can affect the photoemitted electrons. For example, the peaks do not result from some sort of resonant-transmission effect that gives a particularly high probability of escape at some final energy. Such an effect would produce structure stationary in final energy position, in contradiction to our results. Also, the peaks do not result from a fixed energy-loss mechanism operating as electrons excited in the Ni pass through the surface region. In that case, electrons in these peaks would escape at higher energy as this loss mechanism is suppressed. No such effect is observed. Thus we conclude that the peaks result from an increase in the optical absorption.

We observed in the preceding section that the strength of peaks 4 and 6 seem to be proportional to the number of electrons in the cesium layer. Despite this fact, our data strongly indicate that the additional absorption

cannot be associated with optical excitation in the cesium layer. In the first place, too many electrons are involved. Assuming that the optical-absorption parameters of bulk cesium apply to single monolayers of cesium, the total number of electrons produced by absorption in the cesium layer is too small by a factor of 5 or more to account for the electrons in peaks 4 and 6.²⁷

In the second place, the energy position of the cesium-related peaks are not consistent with absorption in an isolated cesium layer. The energy states associated with cesium lie in a band extending $\lesssim 1.7$ eV below the Fermi level.²⁶ 1.7 eV is the width of the band below the Fermi level for bulk cesium and should be a maximum for the width of the filled band of a single cesium layer since the spread of allowed energies for a single adsorbed atom has been calculated to be about 1 eV.³⁰ Therefore, electrons with initial states in the cesium must suffer fixed energy losses to appear in peaks 4 and 5.4 eV below the upper edge of the PED. The plasma losses associated with cesium are $\lesssim 2.85$ eV, and, as we have seen in the previous section, come into play at larger cesium coverages. In the absence of other fixed energy losses associated with cesium, we must seek fixed energy losses associated with the Ni substrate of the cesium-nickel system.

C. Clean-Surface Results

Similar problems are met in trying to explain the anomalous peak at -4.5 eV observed by many workers on more or less clean surfaces. Too many electrons are involved to explain the structure in terms of emission from surface states. Moreover, the peak is not observed with other substrates having similar surface contaminants. Also, Spicer⁷ has shown that the peak in the photoemission is consistent with structure in the optical conductivity of Ni which measures the optical absorption in that material. Nevertheless, a variety of experimental results indicates that the strength of the peak at -4.5 eV is closely related to the surface condition. Hence we seek an explanation whereby the surface condition can modify absorption occurring below the surface. It must also provide an energy-loss mechanism that results in the displacement of a large percentage of the excited electrons to lower-energy states.

D. Surface Plasma Excitations

We propose the following explanation for our results. It accounts in a qualitative fashion for the data and has the additional virtue that its validity can be checked by independent experiments. Consider first electrons in the peak at -4.5 eV in the PED from clean Ni surfaces. Our experimentally based conclusions about this peak are summarized in statements (1)-(4) of

³⁰ J. W. Gadzuk, *Surface Sci.* **6**, 133 (1967).

Sec. III E. We suggest that these electrons are excited from initial states in the d band of Ni. The excitation mechanism involves the loss of a fixed energy of about 4.0 eV to a surface plasmon, so that electrons escape the surface with a fixed energy loss.

The deposition of monolayer coverages of cesium on the surface produces the changes in PED summarized in statements (5)–(10) of Sec. III E. We argue that these effects are produced when the cesium deposition modifies and enhances the surface plasma loss mechanism either by changing the boundary conditions on the complex dielectric constant at the surface or by increasing the coupling of the light to the surface plasma waves by increasing the surface roughness. Several aspects of the proposal are discussed below.

We may inquire whether our interpretation is consistent with the experimentally determined dielectric constants for Ni. We recall first the behavior of the dielectric constants near plasmon energies.^{28,29} The condition on the complex dielectric constant determining the existence of an undamped bulk plasma excitation is that

$$\epsilon = \epsilon_1 + i\epsilon_2 = 0 \quad (4)$$

and on an undamped surface plasmon is that

$$\epsilon + \epsilon' = 0, \quad (5)$$

where ϵ' is the dielectric constant of the medium adjacent to the solid surface. For the free-electron case, $\epsilon_2 = 0$ in the region of the plasmon excitations. The bulk plasma excitation then occurs where $\epsilon_1 = 0$, and the surface plasma excitation at the energy occurs where $\epsilon_1 = -\epsilon'$. At a vacuum interface, $\epsilon' = 1$, so that the surface excitation is to be found where $\epsilon_1 = -1$. In real metals where $\epsilon_2 > 0$, but small, conditions (4) and (5) applied to ϵ_1 alone only approximately locate the energy of the plasma excitation, and the finite value of ϵ_2 gives a measure of the damping associated with the decay of the plasmon into single-particle excitations. Ehrenreich and Philipp³¹ have given more detailed criteria for the identification of bulk plasma resonances from the dielectric constant data. Similar criteria may be applied to assist in the identification of surface resonances from such data.

Published experimental values of ϵ_2 for Ni in the region of 4 eV ($\epsilon_2 \simeq 4$) are too large to strongly support our interpretation of the photoemission data, and imply that if a plasmon excitation exists, it is a strongly damped oscillation closely coupled to one-electron transitions. ϵ_1 , on the other hand, increases to a value of approximately -1 near 4 eV. Thus its behavior is approximately that expected in the region of a surface plasma excitation.³²

³¹ H. Ehrenreich and H. R. Philipp, in *Proceedings of the International Conference on the Physics of Semiconductors* (The Institute of Physics, University of Reading, Berkshire, England, 1962), p. 367.

³² H. Ehrenreich, H. R. Philipp, and D. J. Olechna, *Phys. Rev.* **131**, 2469 (1963).

Similar behavior of the dielectric constants are observed in Cu. If our suggested interpretation of our photoemission data is correct, a similar interpretation may account for structure in the PED of copper that occurs about 4.0 eV below the d -band peak.³³

It is well known that surface plasma waves do not couple directly to light incident normal to the surface. Coupling can be provided, however, by surface irregularities or impurities or by simultaneous one-electron transitions that serve to satisfy momentum-conservation requirements. We assume in our case that an interband transition of energy $h\nu - h\omega_s$, where $h\nu$ is the photon energy and $h\omega_s$ the plasmon energy, accompanies the plasmon excitation and provides the necessary coupling to the plasmon mode. Surface irregularities could also play a part.

Fields associated with surface plasma waves penetrate into the solid by distances of the order of the plasma wavelength. Since the wavelength for stable plasma oscillations range upward from distances of a few angstrom, most surface plasma waves can couple to interband transitions occurring within the escape depth for photoexcited electrons in Ni, which has been shown⁴ to be approximately 20 Å.

A monolayer of cesium can most plausibly modify the strength of the plasmon-induced absorption by changing the boundary conditions (5) determining the existence of the surface plasma excitation, perhaps by reducing the damping of the plasma wave. An increase in surface roughness due to the formation of islands of cesium might also play a part.

It seems possible that these qualitative features of surface plasma waves can provide a means of explaining several features of the experimental results that are extremely difficult to account for in any other way. First, the optical constants of Ni give some hope that a surface plasma excitation of the proper energy (~ 4 eV) can exist at the Ni surface. Second, plasmon-assisted interband transitions provide a mechanism by which changes in the surface condition produced by very small amounts of *surface contaminants* can profoundly alter the total absorption occurring *inside the Ni* within the escape depth for photoexcited electrons.

Much additional speculative discussion could be devoted to this proposed explanation as it relates to details of the data presented here. Questions that might be considered are:

(1) For electrons emitted into the cesium-related peaks, are initial states in the cesium or in the Ni substrate.

(2) Does the double peak associated with the cesium layer reflect a splitting of the clean-surface peak due to interference effects between plasma excitations in the

³³ C. N. Berglund, in *Proceedings of the Symposium on Optical Properties and Electronic Structure of Metals and Alloys*, edited by F. Abeles (North-Holland Publishing Co., Amsterdam, 1966), p. 285.

Ni and the cesium layer, or does it reflect a sharpening of a single-resonance frequency that allows us to resolve peaks in the density of initial states for the interband transition that accompanies the plasma excitation?

(3) Is the ordering of the cesium layer, reflected in the LEED measurements, important to the observed structure in the PED? Data taken on another surface of Ni may provide further information on this point.

(4) What is the mechanism by which the cesium layer enhances the absorption?

These and other such questions may prove useful for guiding further discussion and experiments, but are less important than experiments designed to check the central elements of the proposed explanation. These are (a) that the surface plasma excitation exists, (b) that it provides an efficient optical-absorption mechanism in

the surface region, and (c) that its character can be modified by changing the surface conditions and in particular by depositing cesium on the surface. It should be possible to confirm the existence of the surface plasma excitation by measuring the energy losses of relatively slow electrons (<1000 eV volts) reflected from thin Ni films. Such measurements have been used extensively in the past to study surface plasma excitations.^{28,34} If the plasma excitation contributes to absorption, and its character varies with surface condition, the magnitude of structure in the optical conductivity that has been associated with the anomalous peak at -4.5 eV should also vary with surface condition, and, in particular, with the deposition of cesium.

³⁴ L. K. Jordon and E. J. Scheibner, *Surface Sci.* **10**, 373 (1968).

Self-Consistent Solution of the Anderson Model*

ALBA THEUMANN†

Belfer Graduate School of Science, Yeshiva University, New York, New York 10033

(Received 29 May 1968)

The Anderson model is studied by means of retarded double-time Green's functions in the limit $U \rightarrow \infty$. Using a truncation procedure and solving self-consistently for the averages, an integral equation for the transition matrix is derived. The exact solution to this equation can be found by analytic methods and is very similar to the solution to the s - d exchange model. The known perturbation result for high temperatures is also obtained from our integral equation.

INTRODUCTION

SOME time ago a model Hamiltonian was introduced by Anderson to describe a localized state of an impurity in a metal.¹ Kim² went beyond the Hartree-Fock approximation used by Anderson and looked for a solution by means of the double-time Green's-function method.³ However, the solution found by Kim is essentially equivalent to perturbation theory and diverges at the Fermi surface at low temperatures.

Our self-consistent treatment of Anderson's Hamiltonian is very similar to that used by Bloomfield and Hamann⁴ in the solution of Nagaoka's⁵ equations for the s - d exchange model.

In Sec. I we look for the equations of motion of the double time, retarded Green's functions, and we solve

for the one-particle Green's functions for conduction electrons, after making the system of equations finite by a truncation procedure. We find our equations to be very similar to Nagaoka's equations in the limit $U \rightarrow \infty$. We derive an integral equation for the transition matrix, of the same type as that discussed in Refs. 6 and 7, and we solve the integral equation with the method of Bloomfield and Hamann. We show how the known perturbational result can be obtained after expanding the t matrix in a power series in $\rho V^2/|\epsilon_d|$, valid for $T > T_K$.

In Sec. II we calculate an approximate expression for the low-temperature resistivity, finding a result very close to that of Hamann⁷ except for the presence of a term of order V^2 due to the finite lifetime of the electrons at the d level.

I. DERIVATION OF AN INTEGRAL EQUATION FOR THE TRANSITION MATRIX

Anderson's model Hamiltonian is

$$H = \sum_{k,s} \epsilon_k a_{ks}^\dagger a_{ks} + \sum_s \epsilon_d d_s^\dagger d_s + U d_\uparrow^\dagger d_\downarrow d_\downarrow^\dagger d_\uparrow + V \sum_{k,s} (a_{ks}^\dagger d_s + d_s^\dagger a_{ks}), \quad (1)$$

⁶ D. Falk and M. Fowler, *Phys. Rev.* **158**, 567 (1967).

⁷ D. R. Hamann, *Phys. Rev.* **158**, 570 (1967).

* Supported by U. S. Air Force Office of Scientific Research Grant No. 1075-66.

† Present address. Institutt for Teoretisk Fysikk, N. T. H. Trondheim, Norway.

¹ P. W. Anderson, *Phys. Rev.* **124**, 41 (1961).

² D. J. Kim, *Phys. Rev.* **146**, 455 (1966).

³ D. N. Zubarev, *Usp. Fiz. Nauk* **71**, 71 (1960) [English transl.: *Soviet Phys.—Usp.* **3**, 320 (1960)].

⁴ Ph. E. Bloomfield and D. R. Hamann, *Phys. Rev.* **164**, 856 (1967). We thank Professor Horwitz for pointing out this reference before its publication.

⁵ Y. Nagaoka, *Phys. Rev.* **138**, A1112 (1965).